Development of a New Beam-Energy-Spread Monitor Using Multi-Stripline Electrodes

Tsuyoshi Suwada (e-mail:tsuyoshi.suwada@kek.jp),
Masanori Satoh and Kazuro Furukawa,
Accelerator Laboratory,
High Energy Accelerator Research Organization (KEK),
1-1 Oho, Tsukuba, Ibaraki 305-0801, Japan

KEKB Accelerator Complex

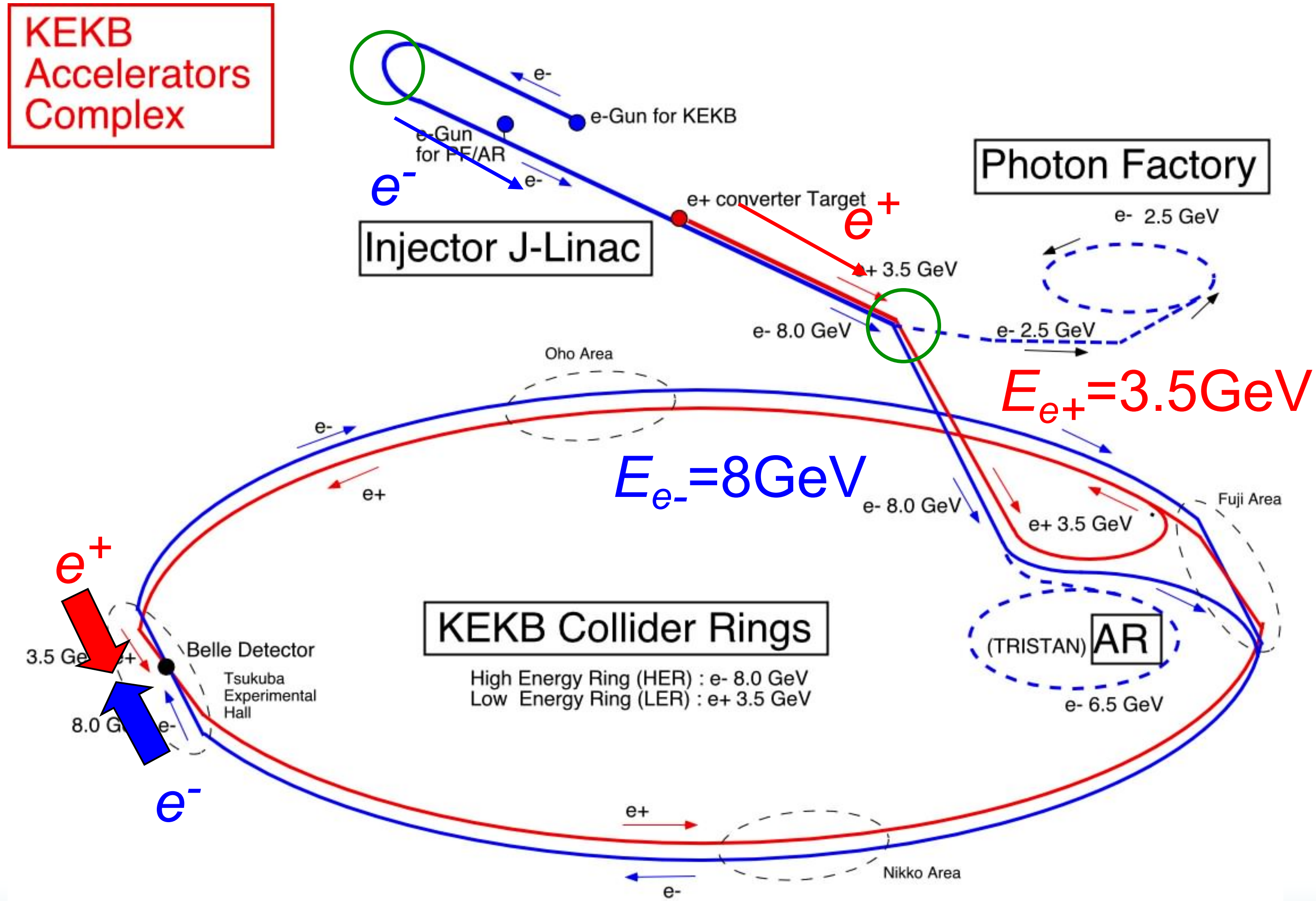

Introduction

Purpose

Well-controlled operation of the *KEKB injector linac* is strongly required

- for keeping the injection rate as high as possible,
- and for maintaining stable operation.

Beam Feedback Controls

- Beam position feedback [*LINAC2000*, pp.633-635]
- Beam energy feedback [*ICALEPCS'99*, pp.248-250]
- *Beam energy-spread feedback*

Motivation

- A nondestructive energy-spread monitor contributes toward further stable operation/injection of the linac.

→ We developed a new beam energy-spread monitor with multi-stripline electrodes.

Beam Energy-Spread Monitor with Eight Stripline-Type Electrodes

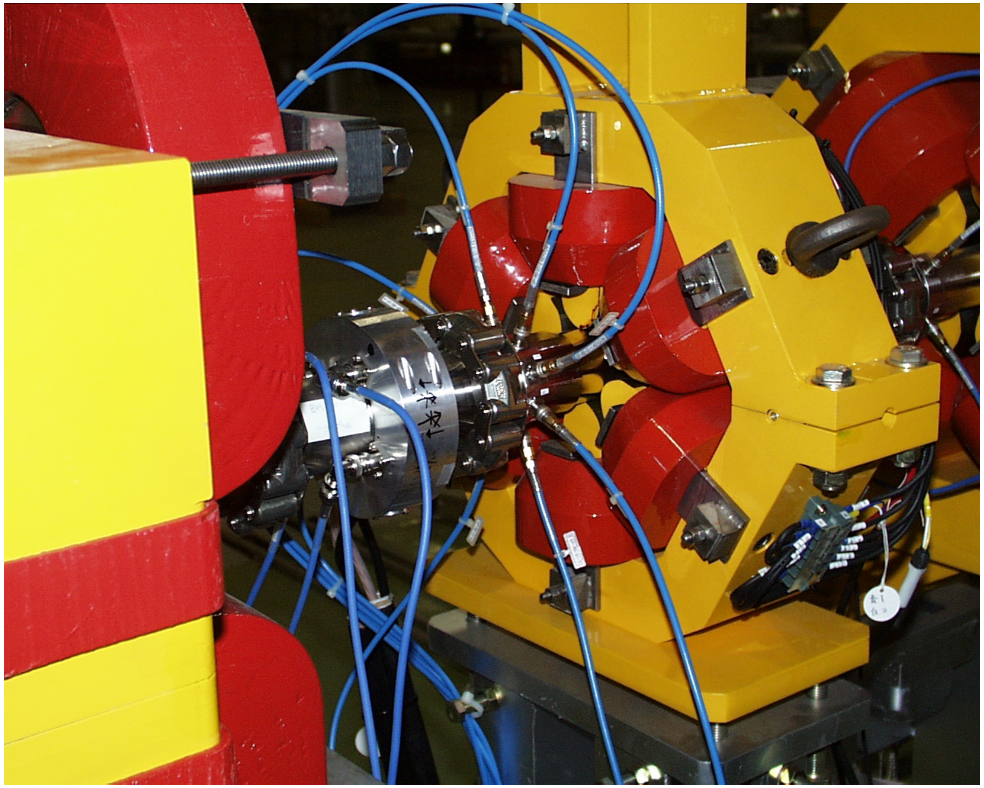

- This work was strongly motivated by a pioneering work of R. H. Miller, et al. [*HEAC'83*, pp.602-605].

→ They showed that a stripline-type BPM with four pickups could be utilized as a nonintercepting emittance monitor.

- Also our previous work using similar stripline-type BPMs [*Jpn.J.App.Phys.* 40 (2001), pp.890-897] demonstrated that the higher-order (second- and third-order) moments of an electron beam were directly measured depending upon the transverse beam sizes.

Multi-Stripline Energy-Spread Monitor: Mechanical Design Parameters

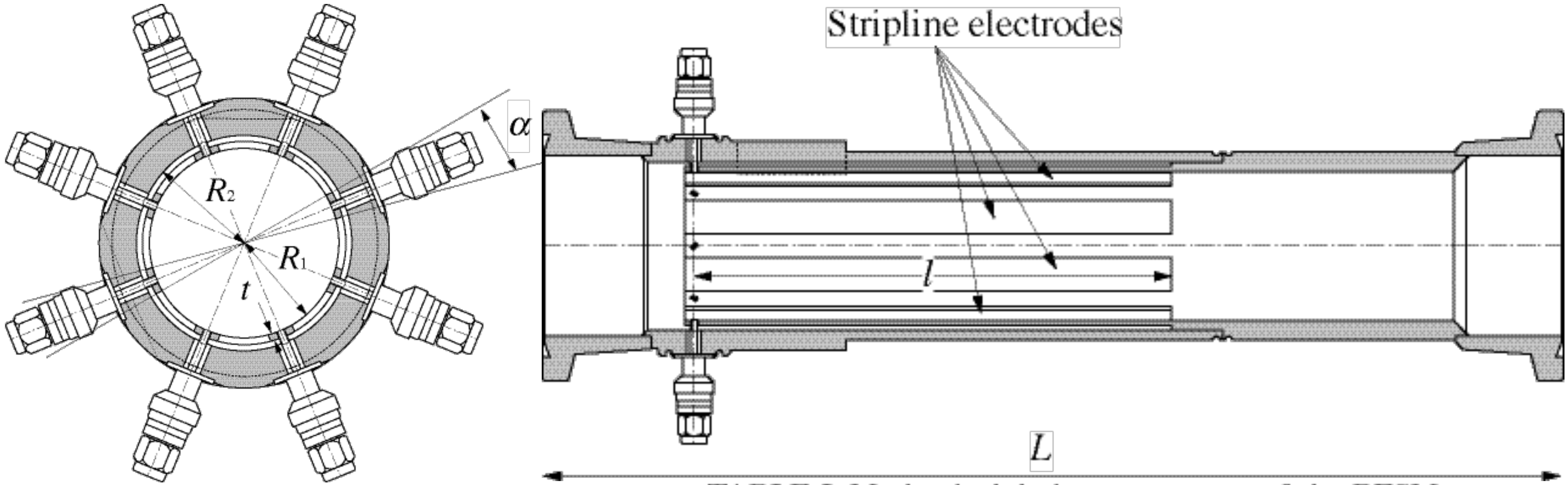

TABLE I: Mechanical design parameters of the BESM.

Mechanical parameter	
Innner radius R_1 (mm)	20.6
Outer raidus R_2 (mm)	23.4
Electrode angular width α (deg)	15
Electrode thickness t (mm)	1.5
Electrode length l (mm)	132.5
Total length L (mm)	283

Multipole Analysis of the Electromagnetic Field Generated by a Charged Beam

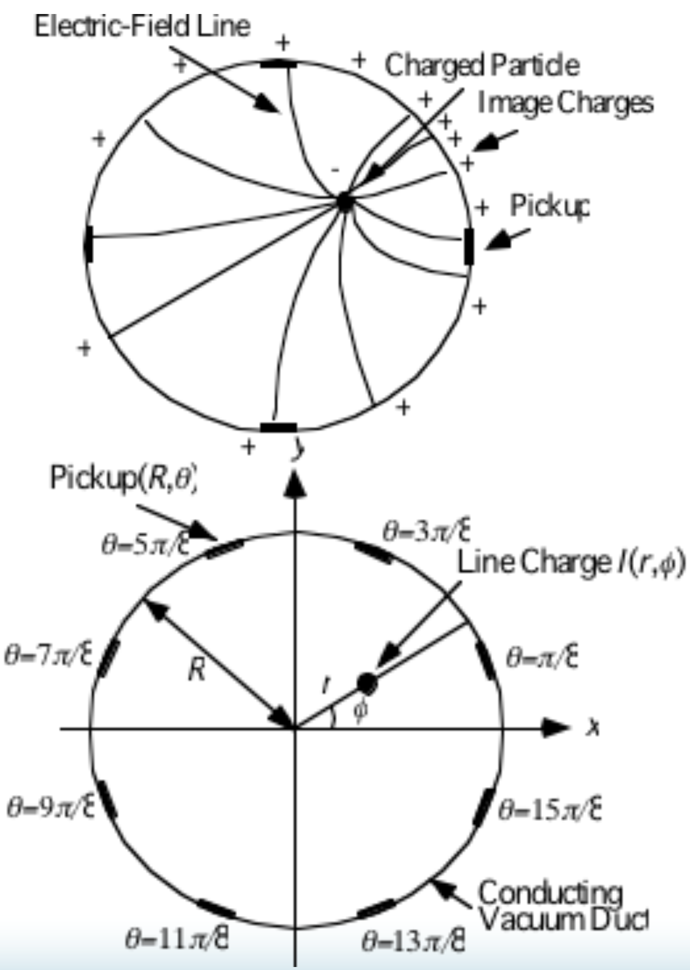

- The image charge density distribution by a line charge for a conducting round duct is formulated by,

$$j(r,\phi,R,\theta) = \frac{I(r,\phi)}{2\pi R}\left[1 + 2\sum_{n=1}^{\infty}\left(\frac{r}{R}\right)^n \cos n(\theta-\phi)\right].$$

- Assuming the transverse r-distribution $\rho(r)$ of a traveling charged beam, the total image charge J is formulated by,

$$J(R,\theta) = \int_0^R \int_0^{2\pi} j(r,\phi,R,\theta)\rho(r)\, r\, dr\, d\phi.$$

- It is easily expanded by the power series,

$$J(R,\theta) = \frac{I_b}{2\pi R}\left\{1 + \frac{2}{R}\left[\langle x\rangle\cos\theta + \langle y\rangle\sin\theta\right]\right.$$
$$+\frac{2}{R^2}\left[\left(\langle x^2\rangle - \langle y^2\rangle + \langle x\rangle^2 - \langle y\rangle^2\right)\cos 2\theta + 2\left(\langle xy\rangle + \langle x\rangle\langle y\rangle\right)\sin 2\theta\right]$$
$$\left. + \text{higher orders}\right\}$$

Multipole Analysis of 8-Electrode BESM

The multipole moments are defined by using the pickup voltages(V_i)

- for the 1st-order (*dipole*) moments,

$$J_{dx} = \frac{\langle x \rangle}{R} = \int_0^{2\pi} J(R,\theta)\cos\theta d\theta \int_0^{2\pi} J(R,\theta) d\theta \approx \frac{\sum_{i=1}^{8} V_i \cos\theta}{\sum_{i=1}^{8} V_i},$$

$$J_{dy} = \frac{\langle y \rangle}{R} = \int_0^{2\pi} J(R,\theta)\sin\theta d\theta \int_0^{2\pi} J(R,\theta) d\theta \approx \frac{\sum_{i=1}^{8} V_i \sin\theta}{\sum_{i=1}^{8} V_i},$$

- and for the 2nd-order (*quadrupole* and *skew*) moments,

$$J_q = \frac{1}{R}\left(\langle x^2 \rangle - \langle y^2 \rangle + \langle x \rangle^2 - \langle y \rangle^2\right) = \int_0^{2\pi} J(R,\theta)\cos 2\theta d\theta \int_0^{2\pi} J(R,\theta) d\theta \approx \frac{\sum_{i=1}^{8} V_i \cos 2\theta}{\sum_{i=1}^{8} V_i},$$

$$J_s = \frac{1}{R^2}\left(\langle xy \rangle + \langle x \rangle\langle y \rangle\right) = \int_0^{2\pi} J(R,\theta)\sin 2\theta d\theta \int_0^{2\pi} J(R,\theta) d\theta \approx \frac{\sum_{i=1}^{8} V_i \sin 2\theta}{\sum_{i=1}^{8} V_i},$$

- the *skew angle* (*x-y coupling*) of the beam is formulated by

$$\theta_{skew} = J_s / 2J_q,$$

- and the *beam energy spread* is also formulated using the optics parameters and transverse emittances by

$$\langle x^2 \rangle - \langle y^2 \rangle \approx \beta_x \varepsilon_x + \left(\eta_x \frac{\Delta E}{E}\right)^2 - \beta_y \varepsilon_y + g$$

where g is the parameter due to the gain imbalance and the geometrical errors of the pickups.

Beam Test at the 180-degree J-arc section of the injector linac

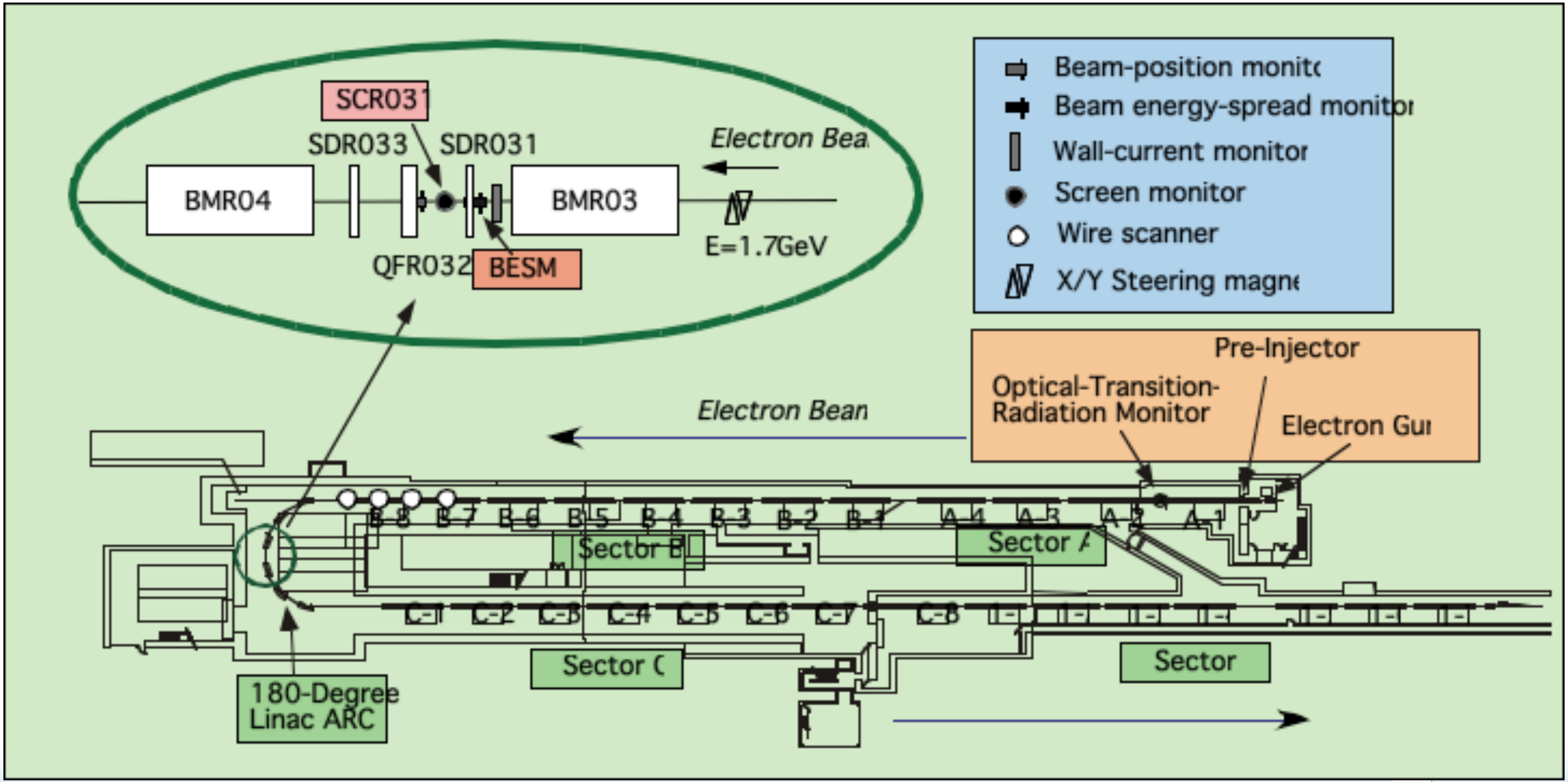

Beam Test:Experiment and beam condition

1. Beam Conditions:

   •single bunch (KEKB) electron and high-current e-/e+ production beam (bunch width=12ps, bunch charge=0.9 and 8nC, repetition rate=25Hz)

   •beam energies (E_b=1.7GeV) at the linac J-arc.

2. Second-order moments (*quadrupole* and *skew* moments) were measured by the BESM depending upon the rf phase of the booster klystron and the transverse beam positions.

3. Beam-size calibration was performed by a fluorescent screen monitor with a high-resolution image processing system.

4. Data-acquisition system of the BESM comprises a signal-digitizing system of a fast oscilloscope(LeCroy WavePro 950) with a sampling rate of 8-GS/s (BW=1GHz) and a PC/Linux-based computer with a Pentium IV microprocessor at 2.2GHz.

Experimental Results:

Variations of the horizontal and vertical beam-position dependence of J_{quad}

Horizontal

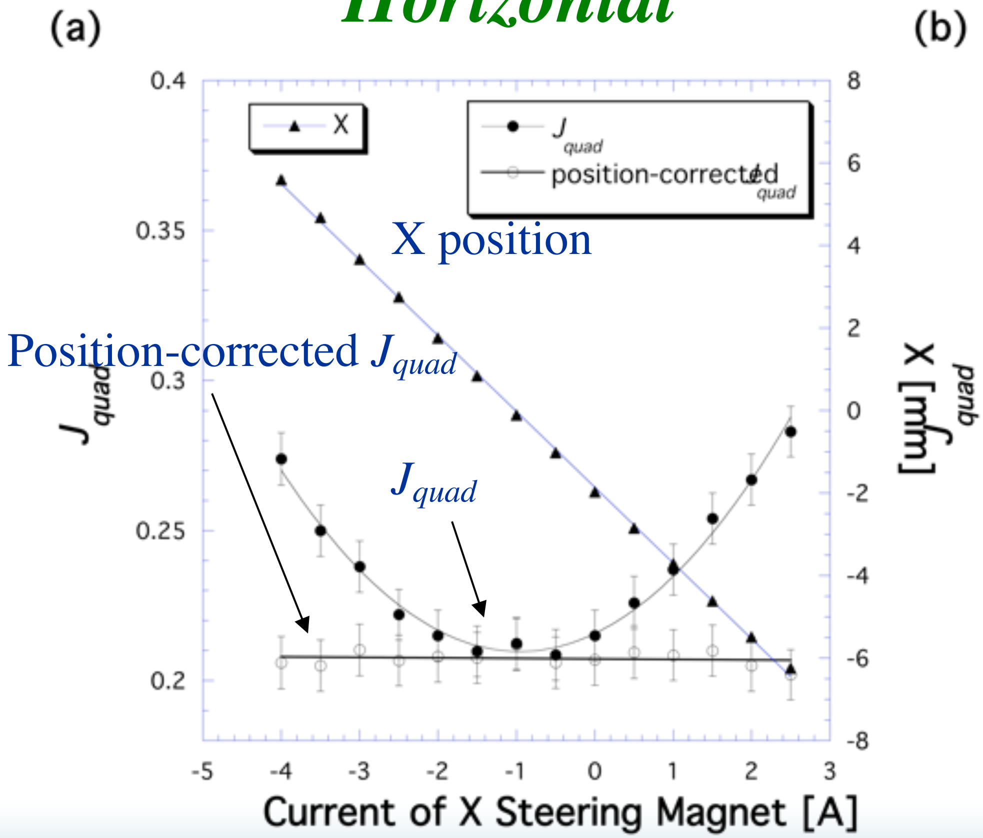

Vertical

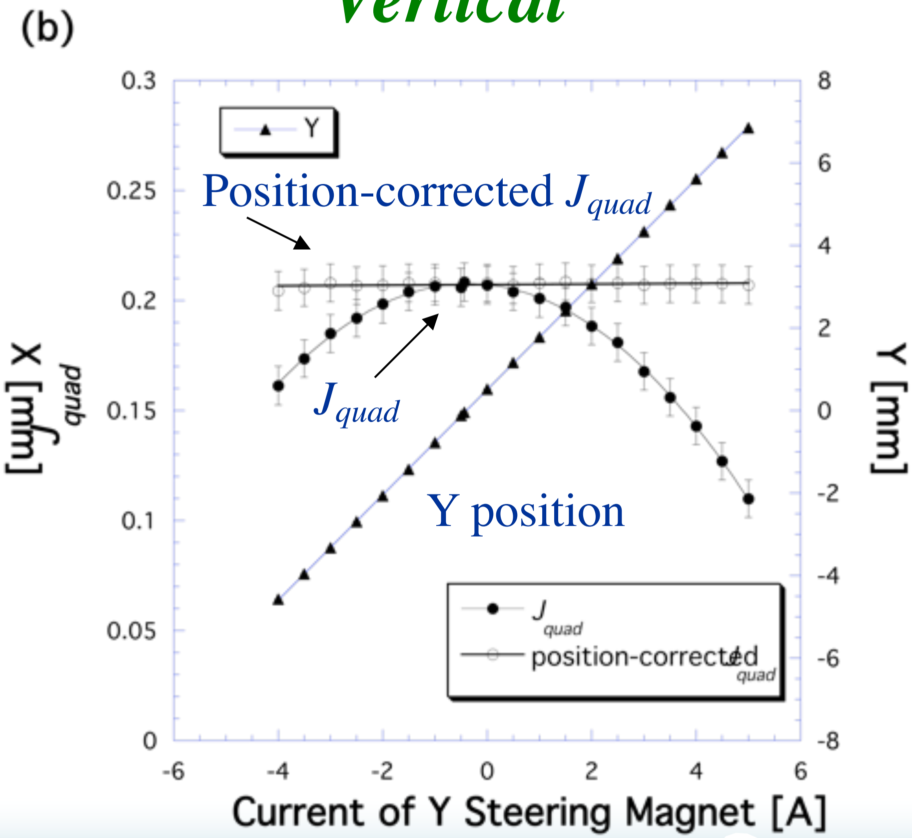

Experimental Results:

Variations of J_{quad} and the energy spread depending on the rf phase (0.9 and 8-nC e- beams)

Variations of J_{quad} / Energy Spread

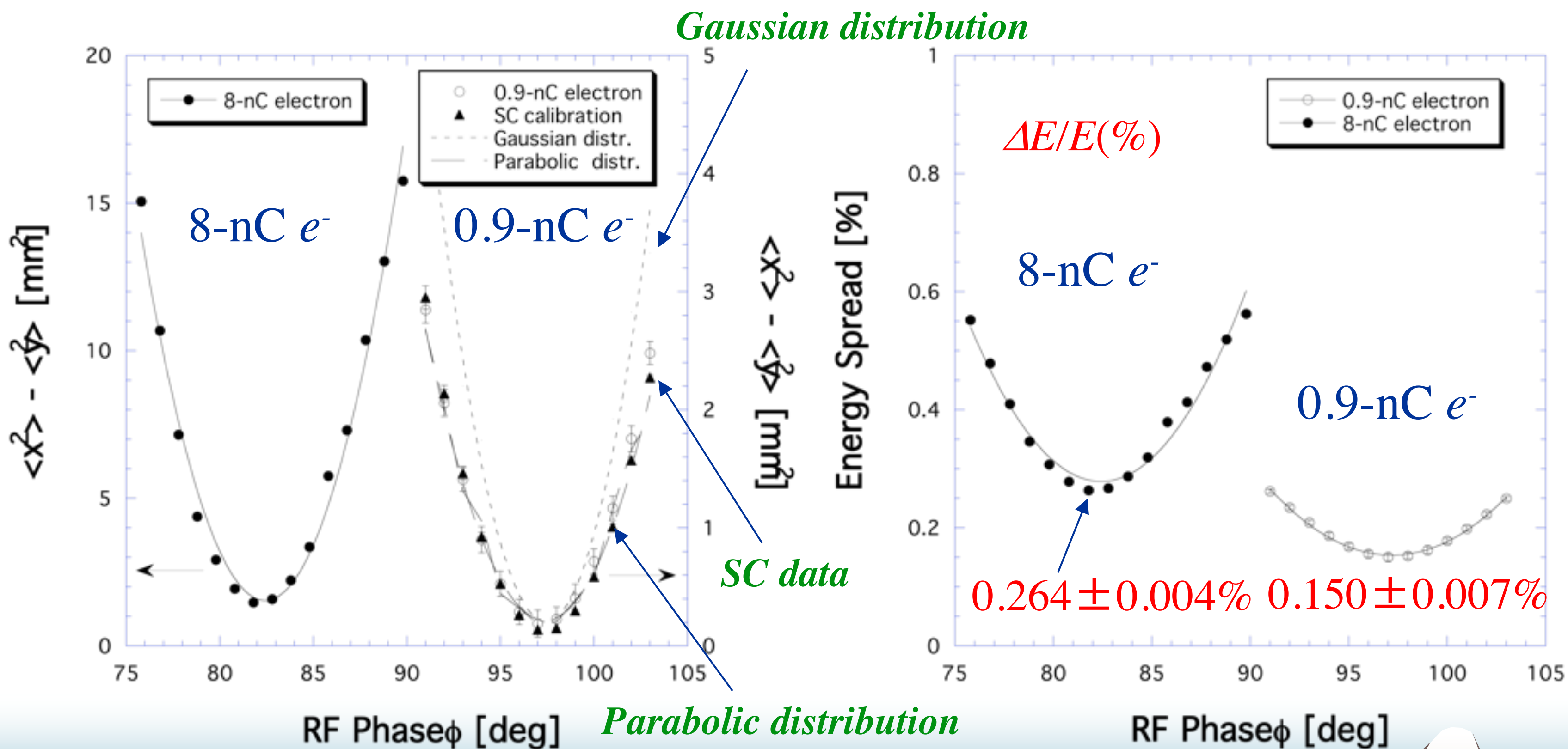

Experimental Results:
Time trend of the quadrupole moment and the rf phase of the booster klystron

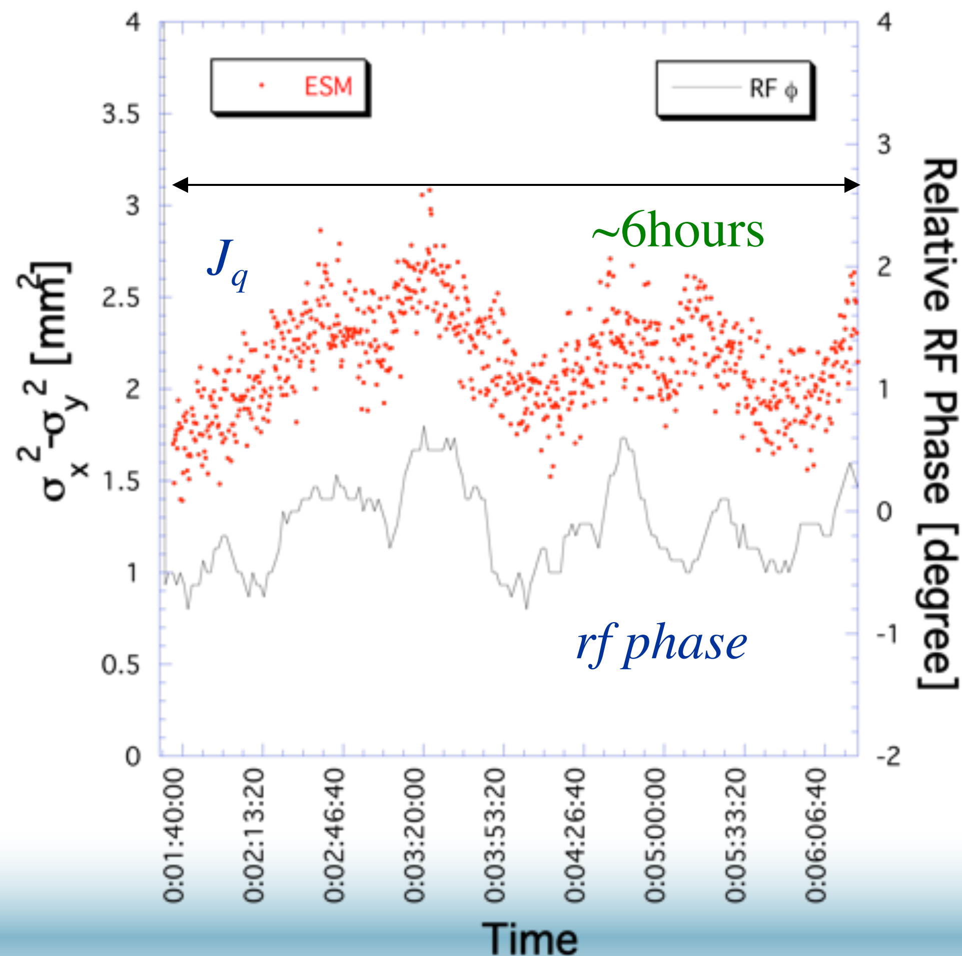

Conclusions

- Result of the beam-size measurement by the BESM is
  - consistent well with that obtained by the fluorescent screen monitor system, and the 2nd-order moments need to be corrected with the transverse beam positions.
- Beam energy spreads were
  - 0.150±0.007% for the 0.9-nC electron beam,
  - and 0.264±0.004% for the 8-nC e- beam, and the resolution is on the order of 10^{-3} depending upon the beam charge and the rf phase.
- Good agreement between the rf phase of the booster klystron and the 2nd-order moment by the BESM for the variation of the time trend is a clear demonstration of the principal function of the BESM, and it is an important step towards the stable operation of the injector linac.
- We have a plan to investigate beam characteristics of two beam bunches in the two-bunch injection scheme.

Multipole Analysis of the Electromagnetic Field Generated by a Charged Beam:

Wall current formula and its multipole expansion(cont'd)

The multipole moments are defined

for the 1st-order moment,

$$\langle x \rangle = \int x j(x,y)\rho(x,y)\,dxdy \quad \langle y \rangle = \int y j(x,y)\rho(x,y)\,dxdy$$

for the 2nd-order moment,

$$\langle x^2 \rangle = \int x^2 j(x,y)\rho(x,y)\,dxdy \quad \langle y^2 \rangle = \int y^2 j(x,y)\rho(x,y)\,dxdy$$

and for the *xy* coupling term,

$$\langle xy \rangle = \int xy j(x,y)\rho(x,y)\,dxdy$$

Multipole Analysis of the Electromagnetic Field Generated by a Charged Beam:

Wall current formula and its multipole expansion(cont’d)

Assuming a gaussian function for the transverse charge distribution, the total image charge is formulated by,

$$J(R,\theta) = \frac{I_b}{2\pi\sigma_x\sigma_y}\iint \frac{j(r,\phi,R,\theta)}{I(r,\phi)} \exp\left[\frac{-(x-x_0)^2}{2\sigma_x^2}\right]\exp\left[\frac{-(y-y_0)^2}{2\sigma_y^2}\right]dxdy$$

$$\begin{aligned} J(R,\theta) \approx \frac{I_b}{2\pi R}\Bigg\{ & 1 + 2\left[\frac{x_0}{R}\cos\theta + \frac{y_0}{R}\sin\theta\right] \\ & + 2\left[\left(\frac{\sigma_x^2-\sigma_y^2}{R^2} + \frac{x_0^2-y_0^2}{R^2}\right)\cos 2\theta + 2\frac{x_0 y_0}{R^2}\sin 2\theta\right] \\ & + 2\left[\frac{x_0}{R}\left(\frac{3(\sigma_x^2-\sigma_y^2)}{R^2} + \frac{x_0^2-3y_0^2}{R^2}\right)\cos 3\theta + \frac{y_0}{R}\left(\frac{3(\sigma_x^2-\sigma_y^2)}{R^2} + \frac{3x_0^2-y_0^2}{R^2}\right)\sin 3\theta\right] \\ & + \text{higher orders} \end{aligned}$$

Multi-Stripline Energy Spread Monitor: Charge Simulation Method

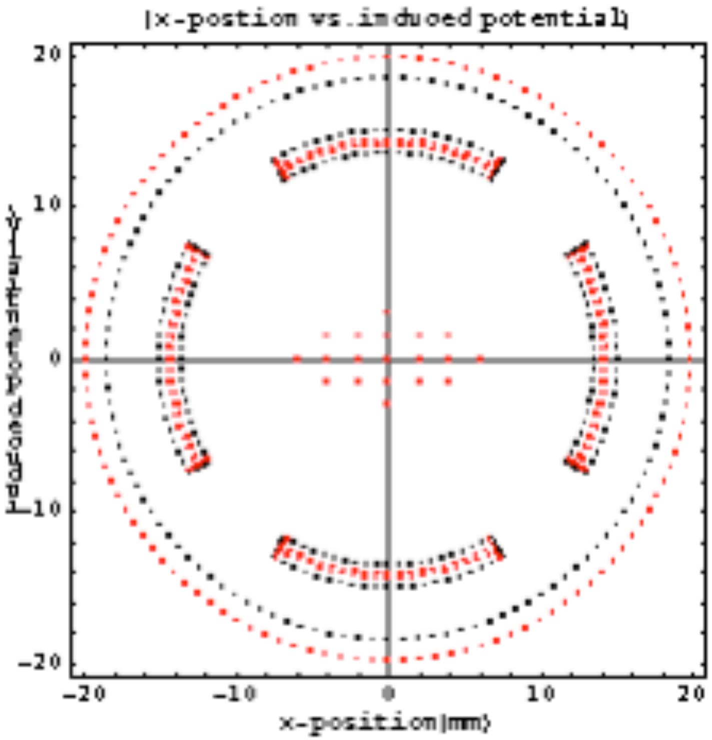

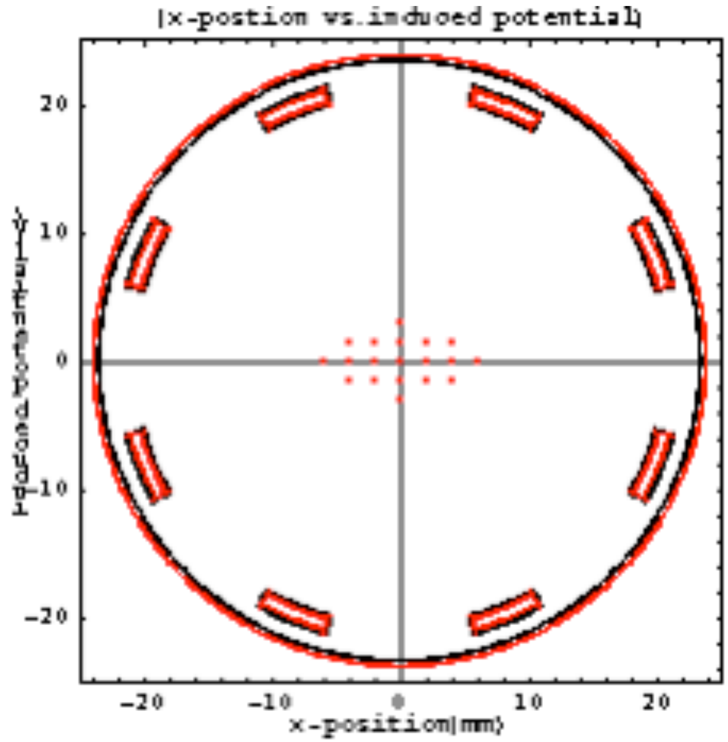

Multi-Stripline Energy Spread Monitor: J_{quad}-Sensitivity Calculation

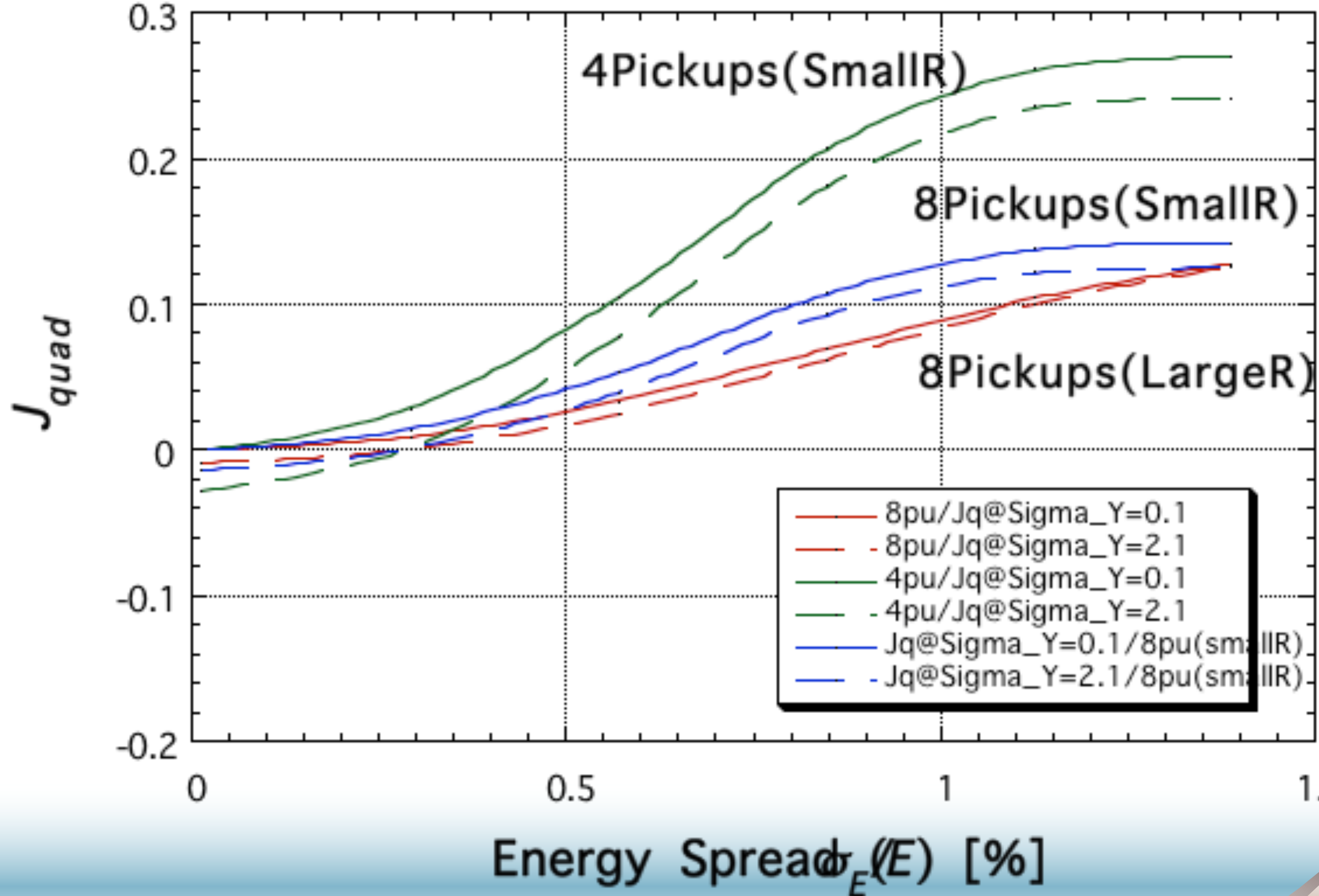

Experimental Results: phase=0deg (0.9-nC e- beam)

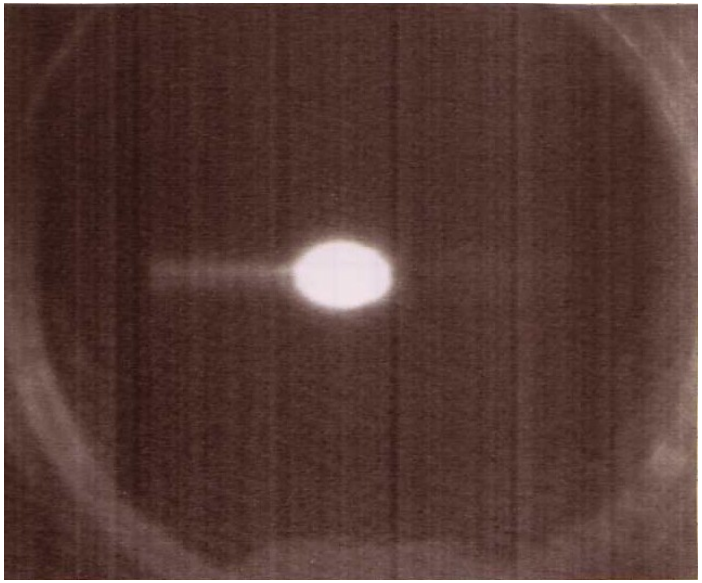

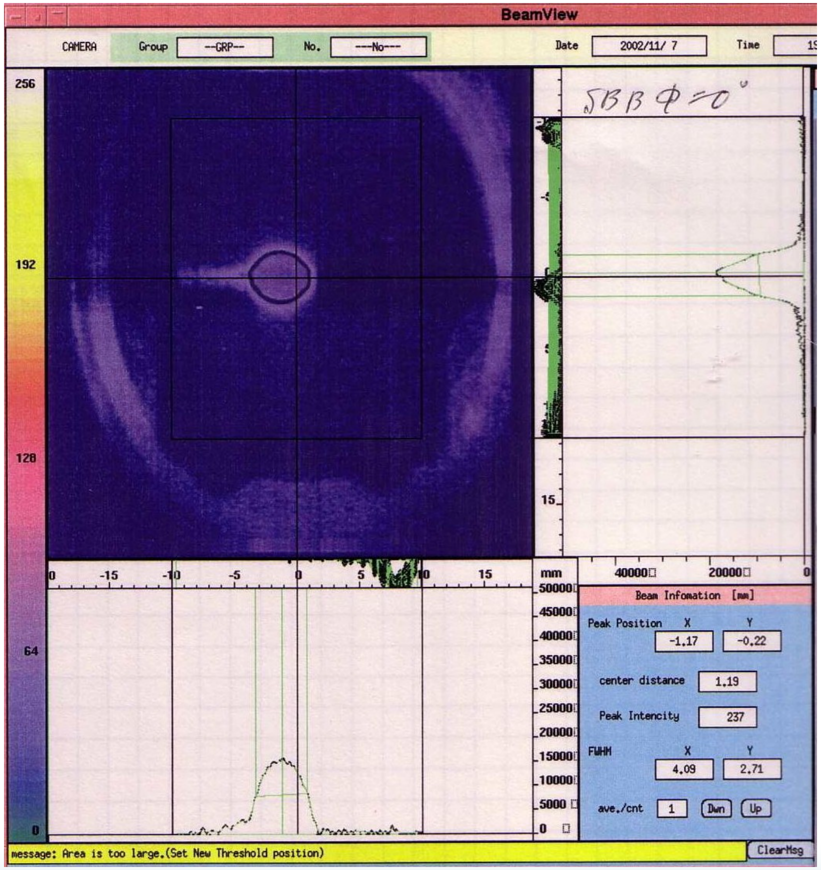

Experimental Results: phase=+3deg (0.9-nC e- beam)

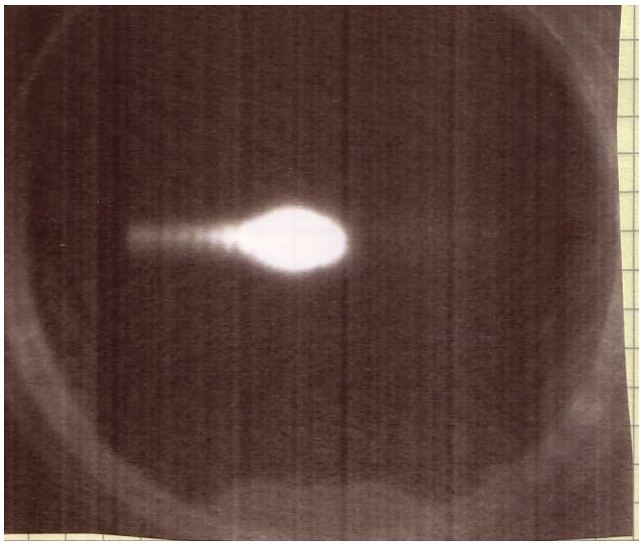

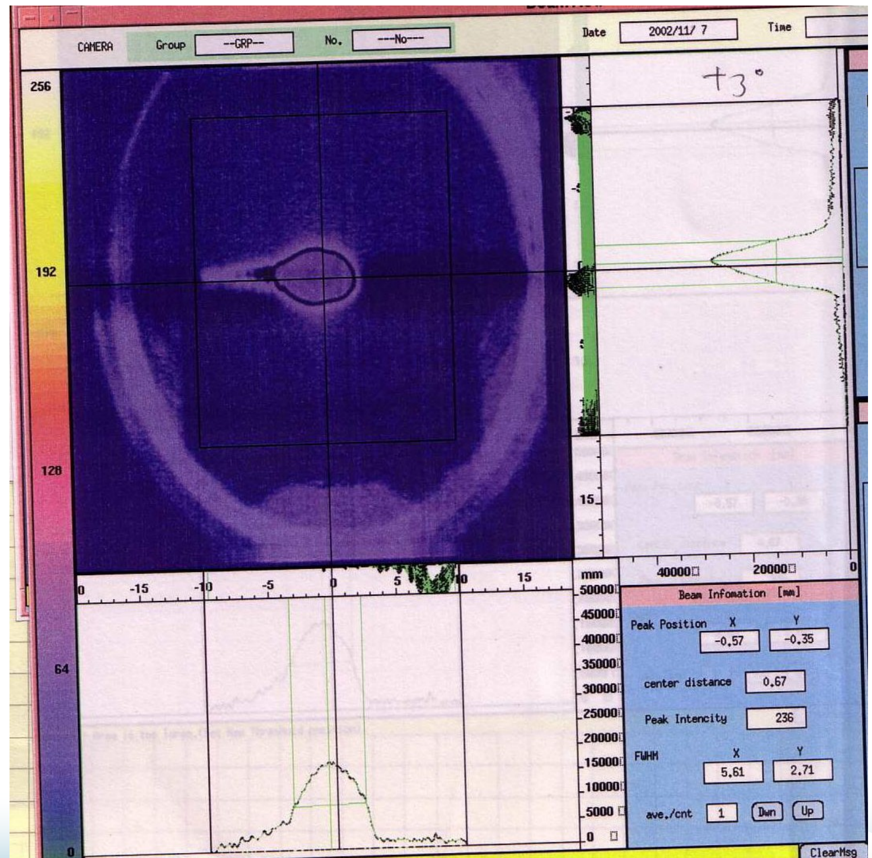

Experimental Results:
Beam-size measurement by the screen monitor system depending on the rf phase (0.9-nC e- beam)

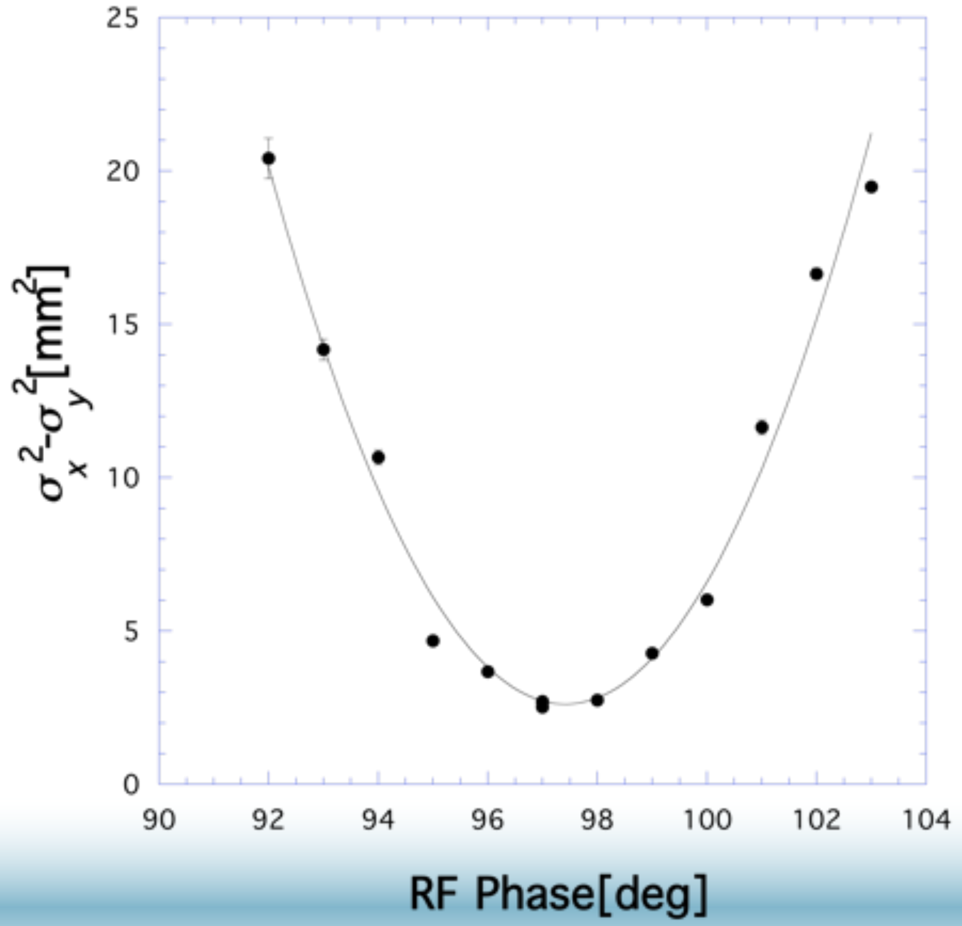

Experimental Results:

Variations of the skew angles depending upon the rf phase (0.9 and 8-nC e- beams)

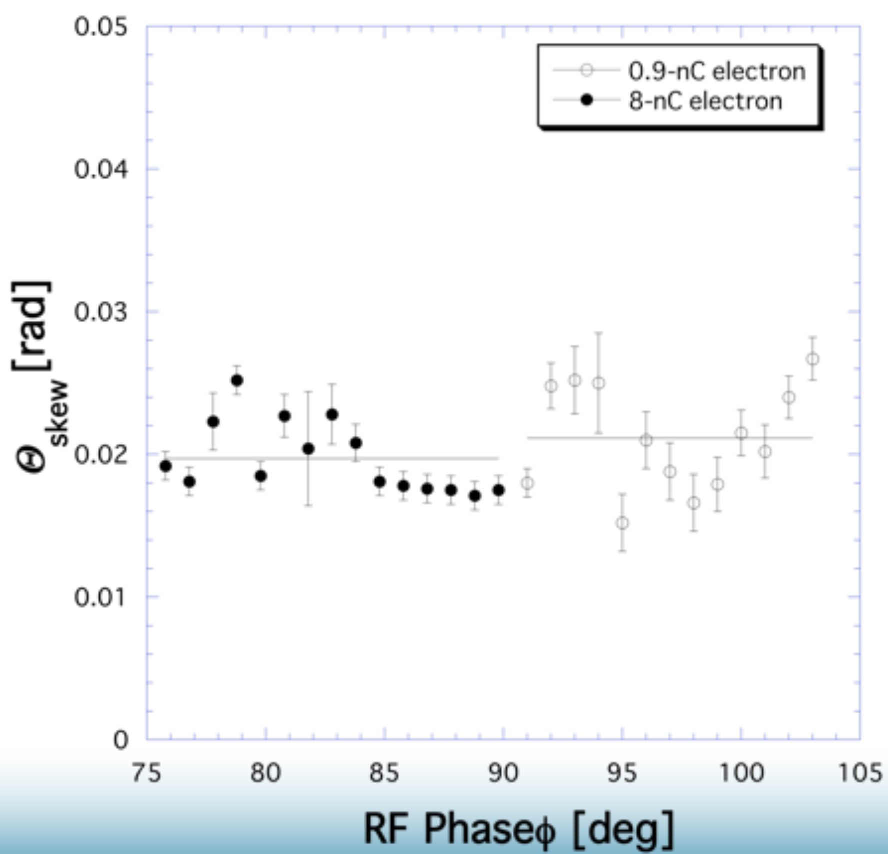

The obtained skew angles in average are

- 21 and 20 mrad for the 0.9- and 8-nC e- beam over the measured region of the rf phase.

Experimental Results:

Variations of J_{quad} and the rf phase resolution depending on the rf phase(0.9 and 8-nC e- beams)

Variations of J_{quad}

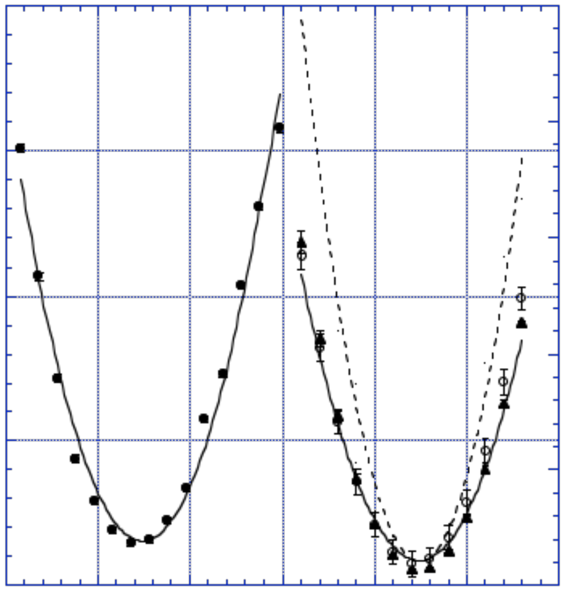

rf phase resolution

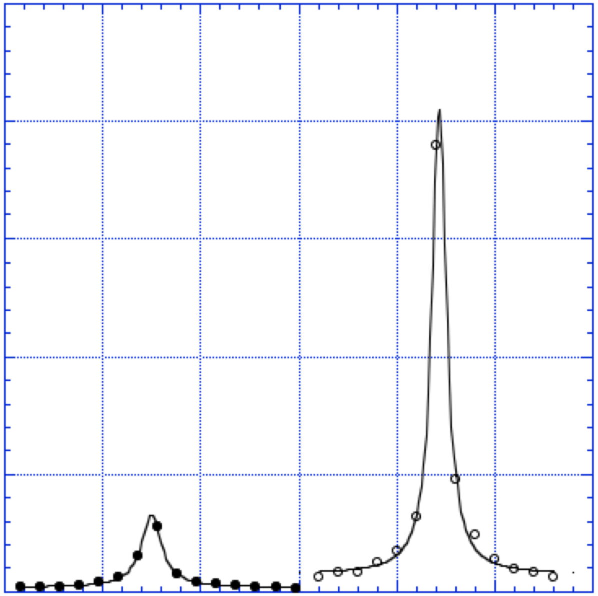

Experimental Results:

Variations of the beam energy spread depending upon the rf phase

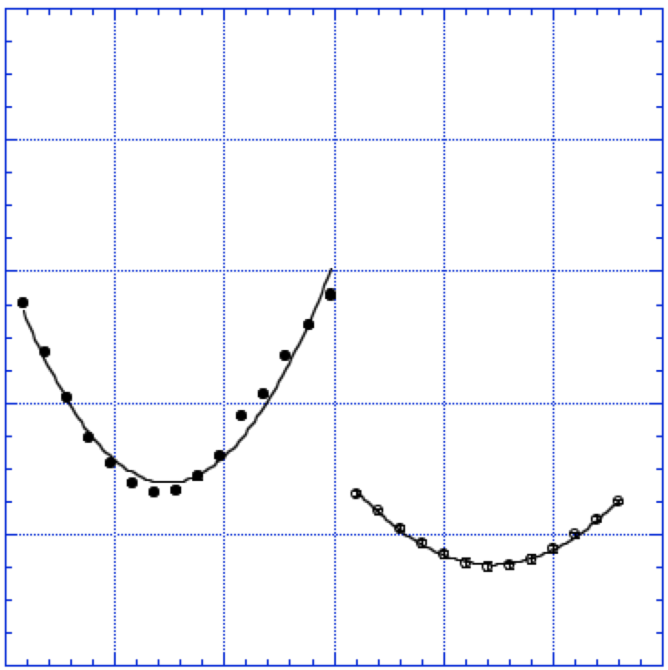

- The obtained beam energy spreads were
  - 0.150±0.007% for the 0.9-nC e-,
  - and 0.264±0.004% for the 8-nC e-/e+ production at the rf phase of the energy-spread minimum

The resolution of the measurement is on the order of 10^{-3} depending upon the beam charge and the rf phase.

Conclusions

- Result of the beam-size measurement by the BESM is consistent well with that obtained by the fluorescent screen monitor system, where the 2nd-order moments need to be corrected with the transverse beam positions.
- RF phase resolutions were
  - less than 1 deg. for the high-current primarly electron(8-nC) beam,

    and less than 1 deg. over the region of ±1 deg. apart from the rf phase at the energy-spread minimum.
- Beam energy spreads were
  - 0.150±0.007% for the 0.9-nC electron beam,
  - and 0.264±0.004% for the 8-nC e- beam, and the resolution is on the order of 10^{-3} depending upon the beam charge and the rf phase.
- Skew angles of the electron beam were
  - 21 and 20 mrad in average over the measured region of the rf phase for the 0.9- and 8-nC electron beam, respectively.